

1                   **Cellulose nanocrystals modification by grafting from ring opening**  
2                                   **polymerization of a cyclic carbonate**

3 Michael Lalanne-Tisné<sup>1,2</sup>, Samuel Eyley<sup>1</sup>, Julien De Winter<sup>3</sup>, Audrey Favrelle-Huret<sup>2</sup>, Wim Thielemans<sup>1\*</sup>,  
4 Philippe Zinck<sup>2\*</sup>

5  
6  
7  
8 <sup>1</sup> Sustainable Materials Lab, Department of Chemical Engineering, KU Leuven, campus Kulak Kortrijk,  
9 Etienne Sabbelaan 53, box 7659, B-8500 Kortrijk, Belgium

10 \*wim.thielemans@kuleuven.be

11  
12 <sup>2</sup> Université de Lille, CNRS, Centrale Lille, Univ. Artois, UMR 8181 - UCCS - Unité de Catalyse et Chimie  
13 du Solide, F-59000 Lille, France

14 \*philippe.zinck@univ-lille.fr

15  
16 <sup>3</sup>Organic Synthesis and Mass Spectrometry Laboratory (S<sup>2</sup>MOs), University of Mons - UMONS, 23 Place  
17 du Parc, 7000 Mons, Belgium

18  
19  
20  
21  
22  
23  
24  
25

26

## 27 **Abstract**

28 Surface modification of cellulose nanocrystals (CNC) by organocatalysed grafting through ring-opening  
29 polymerization (ROP) of trimethylene carbonate was investigated. Organocatalysts including an amidine  
30 (DBU), a guanidine (TBD), an amino-pyridine (DMAP) and a phosphazene (BEMP) were successfully  
31 assessed for this purpose, with performances in the order TBD > BEMP > DMAP, DBU. The grafting ratio  
32 can be tuned by varying the experimental parameters, with the highest grafting of 74% by weight obtained  
33 in smooth conditions, *i.e* at room temperature in tetrahydrofuran with a low amount of catalyst. This value  
34 is much higher than that of typical ring opening polymerizations of cyclic esters initiated from the surface  
35 of cellulose nanoparticles. Additionally, DSC analysis of the modified material revealed the presence of a  
36 glass transition temperature, indicative of a sufficient graft length to display polymeric behaviour. This is,  
37 to our knowledge, the first example of cellulose nanocrystals grafted with polycarbonate arms.

38

## 39 **Keywords:**

40 Cellulose nanocrystals, Organocatalysis, Polycarbonate, Nanocellulose, Ring-opening polymerization

41 Chemical compounds studied in this article:

42 Trimethylene Carbonate (PubChem CID: 123834); 1,5,7-Triazabicyclo[4.4.0]dec-5-ene (PubChem CID:  
43 79873); 4-Dimethylaminopyridine (PubChem CID: 14284); BEMP phosphazene (PubChem CID:  
44 3513851); 1,8-Diazabicyclo(5.4.0)undec-7-ene (PubChem CID: 81184)

45

## 46 **1. Introduction:**

47 Polysaccharides, and in particular cellulose, have experienced a rejuvenation of interest in recent years after  
48 being slowly replaced by petroleum alternatives during the 20<sup>th</sup> century in many applications. With the  
49 increasing concern over sustainability of many aspects of chemistry and materials science, the surge of  
50 interest in these materials is unsurprising as they constitute the bigger fraction of biomass (Habibi, Lucia,  
51 & Rojas, 2010). Cellulose nanoparticles in particular have received a lot of attention due to native cellulose  
52 availability and their interesting properties such as a high aspect ratio, high young modulus, and low density  
53 (Dufresne, 2013). Both cellulose nanofibrils (CNF) and cellulose nanocrystals (CNC) have been widely  
54 studied as fillers for composite materials since the work of Favier *et al.* in 1995 who reported on the first

55 composites reinforced with cellulose nanocrystals. Incorporation of nanocellulose into a polymer matrix has  
56 since been studied extensively and has the potential, especially when combined with biodegradable  
57 polymers, to produce strong yet fully biodegradable materials. To this end, carbonates are of particular  
58 interest, as aliphatic polycarbonates are highly valuable polymers with a very large scope of applications,  
59 most notably in textiles, biomedical applications, microelectronics, and packaging (Yu, 2021). As an  
60 additional benefit to being biodegradable (Artham & Doble, 2008), aliphatic polycarbonates have also been  
61 obtained from renewable sources making them valuable as a potential alternative to petroleum-based  
62 polymers (Helou *et al.*, 2010). To produce high performance composite materials, using nanocellulose  
63 directly as an additive to polymers has proven to give less than ideal results due to the highly hydrophilic  
64 nature of cellulose and its tendency to aggregate. These issues typically lead to a lower than expected  
65 mechanical strength and ductility as these are highly dependent on the dispersion of the reinforcing fibre in  
66 the polymer matrix and on the strength of the interface (Habibi, 2014).

67 To find solutions, a large amount of work has been carried out on the surface modification of cellulose  
68 nanocrystals, typically using the hydroxyl groups (Eyley & Thielemans, 2014) *via* acetylation (Xu, Wu. Z.,  
69 Wu. Q., Kuang, 2020), carbamation (Girouard *et al.*, 2016), esterification (Trinh & Mekonnen, 2018),  
70 etherification (Sahlin *et al.*, 2018), silanization (Anžlovar, Krajnc, & Žagar, 2020), amidation (Lasseguette,  
71 2008), and polymer grafting by different methods. While “grafting to” polymerization, *i.e* the process of  
72 grafting a pre-synthesized polymer chain to the surface of cellulose can be successful (Azzam *et al.*, 2016),  
73 the “grafting from” method is usually the preferred pathway to cellulose modification with polymers as it is  
74 better controlled and avoids problems such as steric hindrance (Wohlhauser *et al.*, 2018). The “grafting  
75 from” approach has been used to couple many types of polymers on cellulose such as *e.g* polylactones  
76 (Habibi *et al.*, 2008; Labet & Thielemans, 2012) and polylactide (Lalanne-Tisné, Mees, Eyley, Zinck, &  
77 Thielemans, 2020). In the case of polymer grafting, the main goal is usually to increase the compatibility  
78 between the cellulose fibres and a polymer matrix (Thielemans, Belgacem, & Dufresne 2006). Lactones and  
79 lactides have received a lot of attention due to their potential in biomedical application (Albertsson &  
80 Varma, 2003) as they can undergo hydrolysis *in vivo*. However, polyester hydrolysis generates carboxylic  
81 acids, which can be a significant drawback (Lendlein & Langer 2002). Polycarbonates demonstrate much  
82 of the same advantages as polyesters when it comes to their degradation *in vivo* (Engler *et al.*, 2013) but  
83 they do not generate acidic products during hydrolysis (Kluin *et al.*, 2009). Despite their potential use,  
84 however, polycarbonate grafting has not seen much attention, with only some work on grafting on cellulose  
85 filter paper (Pendergraph, Klein, Johansson, & Carlmark 2014), synthesis of isosorbide-based  
86 polycarbonates (PC) in the presence of cellulose nanocrystals (Park *et al.*, 2019), and grafting of  
87 poly(trimethylene carbonate) from starch (Samuel *et al.*, 2014). To our knowledge, the grafting of aliphatic  
88 polycarbonates from the surface of cellulose nanocrystals has never been reported before.

89 To exert control over final properties, it is important to have a well-controlled polymerization reaction.  
90 Therefore, the choice of a catalytic system with a high activity and a high level of control is a primary  
91 concern. In the case of aliphatic polycarbonates, ring-opening polymerization (ROP) is currently the leading  
92 approach as it leads to a living polymerization, therefore satisfying the criteria listed before, *i.e* high activity  
93 and high level of control (Jerome & Lecomte, 2008; Penczek, Cypryk, Duda, Kubisa, & Slomkowski, 2007).  
94 State of the art ROP allows for the use of many catalysts, including non-toxic metal centres like zinc.  
95 However the presence of catalyst traces in the material produced is unwanted for many applications, and  
96 metal catalysts are known for being hard to remove completely from polymeric materials (Hafrén &  
97 Córdova, 2005). “Immortal” ring-opening polymerization is an approach that has been used for carbonate  
98 polymerization and which allows for the use of a small amount of catalyst along with a co-initiator in the  
99 form of a protic source. This co-initiator determines the number of chains growing, which gives control over  
100 the chain length no matter the quantity of catalyst used while keeping a high catalytic activity (Helou,  
101 Miserque, Brusson, Carpentier, & Guillaume, 2008). This approach can also be carried out metal free, as  
102 many advances in organocatalysis have led to the emergence of a wide variety of ROP catalysts (Ottou,  
103 Sardon, Mecerreyes, Vignolle, & Taton, 2016). While not all these systems are as efficient as metallic  
104 catalysts, some are very promising and have shown a high degree of control. In the case of aliphatic  
105 carbonates, and in particular trimethylene carbonate (TMC, see Figure 1), base catalysts have been reported  
106 to produce polycarbonates with low dispersity (Kamber *et al.*, 2007). Catalysts of interest include amines  
107 (dimethylethanolamine, 4-dimethylaminopyridine-DMAP), guanidines (1,5,7-triazabicyclo[4.4.0]dec-5-  
108 ene-TBD), amidines (1,8-diazabicyclo[5.4.0]undec-7-ene-DBU), and phosphazenes (2-*tert*-butylimino-2-  
109 diethylamino-1,3-dimethylperhydro-1,3,2-diazaphosphorine-BEMP) among others (Helou *et al.*, 2010;  
110 Lohmeijer *et al.*, 2006). While ring-opening polymerization of trimethylene carbonate with organic catalysts  
111 has been studied extensively in the last decade, small protic molecules such as benzyl alcohol were mostly  
112 used as the co-initiator (Helou *et al.*, 2010). Therefore, using cellulose nanocrystals as the protic source to  
113 obtain a brush copolymer with polycarbonate is an interesting perspective. Understanding of the reaction  
114 and the influence of different parameters would be valuable to increase the general efficiency of polymer  
115 grafting on cellulose, a process with a generally low yield (Lalanne-Tisné *et al.*, 2020). In particular, to our  
116 knowledge, trimethylene carbonate has never been grafted on the surface of cellulose nanocrystals before.  
117 Hence, we report the first synthesis of poly(trimethylene carbonate) grafted cellulose nanocrystals *via* ring  
118 opening polymerization and investigate the influence of experimental parameters in an effort to increase the  
119 grafting efficiency.

120

121

## 122 2. Materials and Methods

### 123 2.1. Materials

124 Sulfuric acid (97%) was obtained from VWR and calcium hydride was purchased from Acros Organics.  
125 Dichloromethane and ethanol (analytical reagent grade) were obtained from Carlo Erba and cotton wool  
126 was obtained from Fischer Scientific. Benzoic acid (99%) and tetrahydrofuran were obtained from Sigma  
127 Aldrich and purified through alumina column (Mbraun SPS). 2-*tert*-Butylimino-2-diethylamino-1,3-  
128 dimethylperhydro-1,3,2-diazaphosphorine (BEMP, 98%) was also obtained from Acros Organics. 1,8-  
129 Diazabicyclo[5.4.0]undec-7-ene (DBU, 99%) was bought from Alpha Aesar and 1,5,7-  
130 Triazabicyclo[4.4.0]dec-5-ene (TBD, >98%) from TCI. BEMP, DBU and TBD were introduced, opened  
131 and stored in a glovebox and used as received.

132 Trimethylene carbonate (TMC, 99.5%) was purchased from Actuell Chemicals and purified by drying over  
133 calcium hydride, filtered under inert atmosphere and then recrystallised. The purified monomer was  
134 subsequently stored in a glovebox. 4-Dimethylaminopyridine (DMAP, 99%) was purchased from Aldrich  
135 and co-evaporated three times with toluene followed by sublimation under vacuum at 85°C and stored in a  
136 glovebox before use.

137 All chemicals were used as received unless stated otherwise.

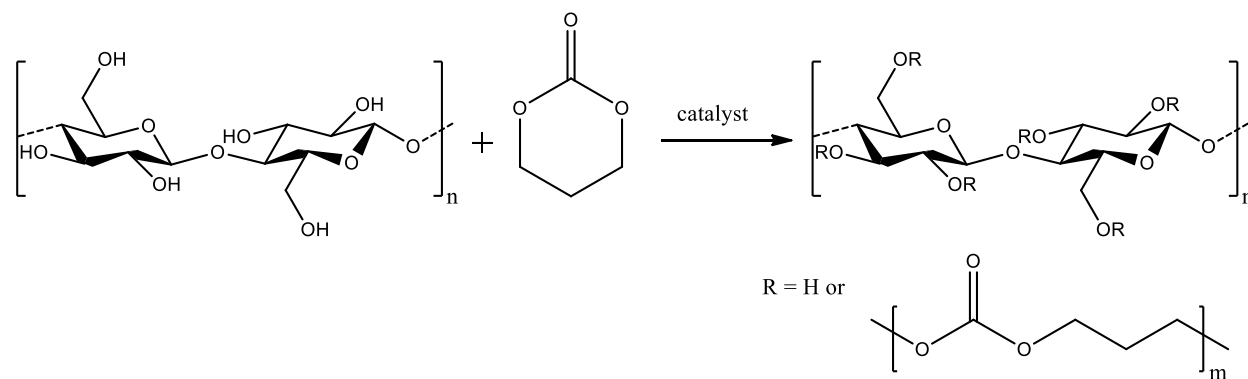
### 138 Preparation of CNCs

139 Cotton nanocrystals were prepared by acid hydrolysis of cotton wool for 35 min at 45°C in a 64 wt% aqueous  
140 H<sub>2</sub>SO<sub>4</sub> solution while stirring constantly (Revol *et al.*, 1992). Deionised water was used to wash the resulting  
141 suspension by three successive centrifugations at 10 000 rpm and 10°C for 40 min, replacing the supernatant  
142 with deionised water each time. Dialysis under continuous tap water flow was then used to remove residual  
143 free acids. After 48 h, the pH of the eluent was checked to be neutral and a homogeneous dispersion of  
144 cotton nanocrystals in water was obtained using a Branson sonicator at 10% amplitude for 2 min. The  
145 dispersion was subsequently filtered over a fritted glass filter no. 2, and stirred overnight with Amberlite  
146 MB-6113 resin to remove non-H<sub>3</sub>O<sup>+</sup> cations. The dispersion was sonicated one last time, frozen in liquid  
147 nitrogen, and freeze-dried using a Heto PowerDry PL6000 apparatus from Thermo Scientific under a  
148 vacuum of 2 bars. In addition to this procedure commonly followed in the literature to prepare cellulose  
149 nanocrystals, a further purification was performed to remove surface adsorbed impurities that adsorb onto  
150 the nanocrystal surface (Labet & Thielemans, 2011). After freeze-drying, the cotton nanocrystals were  
151 Soxhlet extracted for 24h using ethanol as a solvent. The nanocrystals were subsequently dried in a vacuum  
152 oven (0.5 bar) at 50°C and then dried further under ultra-high vacuum (Pfeiffer DCU 100) at 10<sup>-6</sup> bars for 4

153 days. The container used for the drying process was then tightly closed, filled with argon, and placed in a  
154 glovebox.

## 155 2.2. Ring-opening polymerization of TMC on CNC surface

156 All experiments were carried out under inert atmosphere in a glovebox unless stated otherwise.



157  
158 *Figure 1: General reaction scheme of the ring-opening polymerization of trimethylene carbonate co-initiated by hydroxyls present*  
159 *on the surface of cellulose nanocrystals*

160 In a typical reaction, a stir bar was placed in a small reactor, along with a specified amount of CNCs. The  
161 molar ratio used are specified in Table 1 and Table 2 and based of the molecular weight of one glucose ring  
162 bearing one primary OH. THF was added and the mixture was stirred for 30 minutes to disperse the CNCs.  
163 Trimethylene carbonate was then added and left to stir until complete dissolution. Subsequently, the catalyst  
164 was added while stirring and the reactor was placed in an oil bath set at a given temperature. After the  
165 desired duration, the reaction was quenched using benzoic acid and dichloromethane addition, and the  
166 mixture was filtered through a Soxhlet extraction thimble. A sample of the crude mixture was taken for  
167 NMR analysis, and the modified CNCs were purified by Soxhlet extraction twice, first with  
168 dichloromethane (24 hours), and then with ethanol (24 hours).

169 The modified nanocrystals were then dried under vacuum on a Schlenk line (< 1 mbar) for 24 hours.

170 The homopolymer produced as a side reaction was recovered from the first Soxhlet extraction mixture after  
171 evaporation of the dichloromethane.

172 Characterization methods, apparatus, calculation method to determine grafting, conversion and yield, and  
173 additional information about experimental procedures are all available in Supporting Information Appendix  
174 A.

## 175 3. Results and discussion

### 176 3.1. Catalyst screening

Table 1: Ring-opening polymerization of TMC initiated from the surface of CNC in the presence of various organocatalysts at 25°C in THF

Entry	Catalyst	TMC / Catalyst / OH <sup>[a]</sup>	Time (h)	Polycarbonate grafting <sup>[b]</sup> (wt%)	Conversion <sup>[c]</sup> (%)	Grafting Yield <sup>[d]</sup> (%)	M <sub>n</sub> homopolymer <sup>[e]</sup> (g.mol <sup>-1</sup> )	Đ <sub>M</sub> <sup>[f]</sup>
1	Blank	500/0/50	5	2	4	0.3	NA	NA
2	TBD	500/1/50	5	51	99	16.5	19700	1.8
3	BEMP	500/1/50	3	24	45	5.0	35400	1.9
4	BEMP	500/1/50	5	35	52	8.6	33500	1.8
5	BEMP	500/1/50	16	37	52	9.3	33500	1.8
6	DMAP	500/0.5/50	5	13	6	2.4	NA	NA
7	DMAP	500/2/50	5	3	7	0.5	NA	NA
8	DMAP	500/5/50	5	12	6	2.2	2100	1.2
9	DBU	500/1/50	3	18	9	3.5	NA	NA
10	DBU	500/1/50	5	12	8	2.2	NA	NA

[a] Calculated using moles of glucose rings (162.14 g/mol), and considering 1 primary OH per ring [b] Determined by elemental analysis (calculation based on hydrogen content (%H) and carbon content (%C)) and corrected for adsorbed water using TGA. [c] Calculated *via* <sup>1</sup>H NMR to determine monomer/polymer ratio and corrected to include monomer grafted [d] Ratio of initial monomer to monomer grafted. [e] Determined by SEC of homopolymer vs. polystyrene standards and corrected with a correction factor of 0.57, 0.73 or 0.88 based on size measured (Palard *et al.* 2007). [f] Molar mass distribution calculated from SEC of homopolymer.

177 The performances of the different organic catalysts, namely TBD, BEMP, DMAP and DBU (shown in  
 178 Figure 2) to polymerize TMC from the surface of cellulose nanocrystals were evaluated in THF at room  
 179 temperature. The different catalysts were selected from their ability to catalyse ROP of TMC in the presence  
 180 of an alcohol (Helou *et al.*, 2010). The TMC/catalyst/OH ratio was mostly kept at 500/1/50. Table 1 displays  
 181 the most significant results.

182 In the absence of catalyst, significant conversion of the monomer into either grafts or homopolymer was not  
 183 achieved (Table 1, entry 1), showing the clear need to use a catalyst.

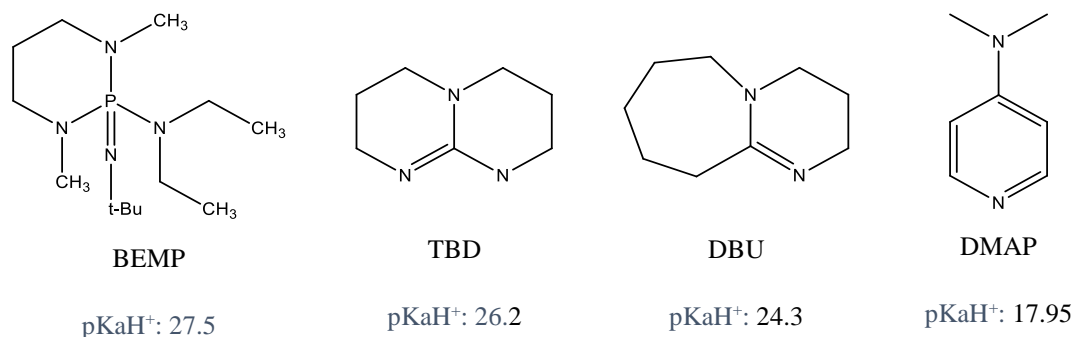


Figure 2: Structure of the organocatalysts used in this study. pKa values in acetonitrile (Ishikawa, 2009; Kaljurand *et al.*, 2005)

184 At a typical ratio of 500/1/50 (TMC/catalyst/OH), TBD was shown to reach full conversion of the monomer  
185 within 5 hours, and resulted in modified CNCs containing of 51% grafted polymer (Table 1, entry 2), a  
186 fairly high value for typical “grafting from” of polymer through ring opening polymerization from the  
187 surface of nanocellulose. Similarly, a significant amount of monomer was converted to homopolymer (yield  
188 of 16% for grafting), which shows an important competition between grafting of the monomer and  
189 homopolymerization. However, it is common for grafting on cellulose to use a large excess of monomer to  
190 increase the amount of grafting at the cost of efficiency (Lalanne-Tisné, *et al.*, 2020; Miao & Hamad, 2016).  
191 Molar mass dispersity of the homopolymer was found at an acceptable value of 1.8 that is significantly  
192 higher than usual values obtained for typical homopolymerizations (Nederberg *et al.*, 2007). The broader  
193 distribution can be explained because it is a side reaction involving water and ethanol as co-initiators that  
194 are still entrapped in the CNCs after purification. In addition, water and ethanol can also be involved in  
195 hydrolysis and transcarbonatation reactions respectively. This can be seen from the MALDI ToF mass  
196 spectra of the precipitated polymer showing the corresponding chain ends (details in Supporting Information  
197 Appendix A).

198 Using similar reaction conditions for BEMP (entries 3-5), a phosphazene catalyst, showed quite different  
199 results. Full conversion was not reached, and after increasing the reaction time from 3 to 5 hours, BEMP  
200 conversion only reached 52%. Further increasing the reaction time to 16 hours did not increase monomer  
201 conversion. Despite the lower conversion values, grafting on cellulose was achieved with this catalyst, and  
202 up to 37% grafts were achieved in the modified CNCs, showing that this catalyst, while less efficient than  
203 TBD using similar parameters, leads to substantial grafting.

204 The reactions conducted with DMAP (entries 6-8) and DBU (entries 9-10) did not perform as well as the  
205 others under the same reaction conditions (room temperature, 5h), with NMR analysis showing very low  
206 conversion. The resulting grafting was rather low for both catalyst (18% maximum) under these conditions,  
207 and no oligomers could be recovered by precipitation to allow for SEC analysis. This is believed to be due  
208 to their likely low average molecular weight.

209 We can try to explain the superior performance of TBD. TBD, unlike the other catalysts tested, possesses a  
210 secondary amine group, giving it great potential for catalysis *via* hydrogen bonding. It is also interesting to  
211 note that unlike DBU, which can operate by a basic and a nucleophilic mechanism, TBD can catalyse  
212 transesterification reactions by dual activation *via* H-bonding (Simón & Goodman, 2007; Stanley *et al.*,  
213 2019). Having a catalyst that can use both mechanisms may result in a better reaction due to the ability of  
214 the catalyst to go in between intermolecular bonding (similarly to how a protic solvent gives a better  
215 dispersion of CNCs). In addition, DBU and DMAP may favour homopolymerization due to their ability to



216 perform a nucleophilic attack on the monomer, which is not the case for the BEMP phosphazene, that leads  
217 to an intermediary grafting ratio.

218 When looking at results for homopolymerization of trimethylene carbonate (Helou *et al.* 2010), it is worth  
219 noting that TBD is also the most active catalyst in bulk, and full conversion is achieved much faster at lower  
220 temperatures when compared to DMAP and DBU. As the work presented here is carried out in solvent but  
221 at room temperature, it is possible that the activity of some of the catalysts (except for TBD) is reduced as  
222 the activation requires more energy. However, further testing at higher temperature with all the catalyst was  
223 not explored as we observed browning of the CNC at temperatures as low as 40°C in the presence of THF  
224 and TBD (see next section).

225 Comparing the pKa of all 4 bases, TBD in acetonitrile does not come up as the strongest base (25.96), with  
226 BEMP having a higher pKa (27.5), despite its superiority when it comes to grafting TMC on cellulose. TBD  
227 is however a stronger base than DMAP and DBU, which could explain partially the better results obtained  
228 when comparing these 3 bases. As for BEMP, it is a much bulkier catalyst, therefore steric hindrance may  
229 be the cause for the lower activity when compared to TMC, in particular for the grafting onto CNC. This  
230 can be exemplified as despite the subpar grafting efficiency on CNCs with BEMP, the extracted  
231 homopolymer showed a higher  $M_n$  than the homopolymer recovered after full conversion with TBD.

232 As the screening of catalysts showed a more efficient grafting with TBD, this reaction was studied further,  
233 in order to assess the influence of the reaction conditions.

### 234 **3.2. Influence of experimental parameters for the TBD catalysed grafting**

235 As the polymerization of TMC has also been performed in bulk (Helou *et al.*, 2010), the grafting reaction  
236 on the surface on CNCs was also carried in bulk as comparison (entry 11, Table 2). Despite  
237 homopolymerization of TMC being very quick under bulk conditions, the reaction with cellulose did not go  
238 to full conversion within an hour. However, the polycarbonate content of modified CNCs did reach 47%, a  
239 value comparable to the content obtained by grafting in THF. The viscosity is a major issue in bulk reactions  
240 as the melted monomer is not a good medium to disperse CNCs, resulting in poor homogeneity of the final  
241 material and a greater difficulty to redisperse the modified cellulose in solvent, rendering its use more  
242 complicated. The high viscosity is also likely a cause for the lower conversion, as the reaction slows down  
243 considerably with homopolymer production. Lastly, the bulk reaction, as expected, shows a much higher  
244 dispersity for the synthesized homopolymer, indicating some loss of control over the polymerization  
245 reaction.

246 THF was used as the main solvent as it had shown to dissolve well TBD, TMC, poly(trimethylene  
 247 carbonate), and to be a good solvent for CNC dispersion. Some other common solvents were assessed, but  
 248 worse results were obtained (additional information in SI).

249 *Table 2: Ring-opening polymerization of TMC initiated from the surface of CNC in the presence of TBD in THF for 5 hours*

Entry	TMC / Catalyst / OH <sup>[a]</sup> T	Polycarbonate grafting <sup>[b]</sup>	Conversion <sup>[c]</sup>	Grafting Yield <sup>[d]</sup>	M <sub>n</sub> homopolymer <sup>[e]</sup>	Đ <sub>M</sub> <sup>[f]</sup>	
	(°C)	(wt%)	(%)	(%)	(g.mol <sup>-1</sup> )		
2	500/1/50	25	51	99	16.5	19700	1.8
11 <sup>[g]</sup>	500/1/50	65	47	33	14.1	11200	3.0
12 <sup>[h]</sup>	500/1/50	25	60	99	23.8	19600	1.9
13	500/1/50	0	54	99	18.7	16500	2.0
14	500/1/50	40	51	99	16.5	14100	2.3
15	500/1/50	60	52	99	17.2	9700	1.8
16 <sup>[i]</sup>	500/1/50	25	7	99	1.2	NA	NA
17	500/1/40	25	49	99	12.2	18700	1.7
18	500/1/30	25	49	99	9.2	23100	1.7
19 <sup>[j]</sup>	500/1/50	25	53	99	17.9	12100	2.0
20	500/2/50	25	9	99	1.6	26700	1.8
21	500/5/50	25	9	99	1.6	2200	1.3
22	500/0.5/50	25	74	99	45.2	7100	1.8
23	500/0.25/50	25	64	78	28.2	11400	1.6
24	250/0.5/50	25	57	99	42.1	11100	1.7
25	125/0.5/50	25	47	99	56.3	4600	1.8
26	62.5/0.5/50	25	23	99	37.9	NA	NA
27	250/1/50	25	50	99	31.8	13700	1.9
28	125/1/50	25	41	99	44.1	12900	1.8

[a] Calculated using moles of glucose rings (162.14 g/mol), and considering 1 primary OH per ring [b] Determined by elemental analysis (calculation based on hydrogen content (%H) and carbon content (%C)) and corrected for adsorbed water using TGA. [c] Calculated *via* <sup>1</sup>H NMR to determine monomer/polymer ratio and corrected to include monomer grafted [d] Ratio of initial monomer to monomer grafted. [e] Determined by SEC of homopolymer *vs.* polystyrene standards and corrected with a correction factor of 0.57, 0.73, or 0.88 based on size measured (Palard *et al.* 2007). [f] Molar mass distribution calculated from SEC of homopolymer. [g] Bulk reaction. [h] Reaction done over 24 hours instead of 5. [i] Reaction performed outside the glovebox. [j] Stirred for 24h and sonicated prior to reaction to maximize dispersion of CNC. NA: not available as oligomers, i.e too short to precipitate in cold methanol

250 As shown previously (entry 11), the polymerization of TMC was total after 5 hours, however a reaction in  
 251 similar conditions was also performed over 24 hours (entry 12) to evaluate the activity of TBD over longer  
 252 period of time, as it has been reported to be capable of depolymerization (Meimoun *et al.*, 2020). In the case  
 253 of poly(trimethylene carbonate) grafted CNCs, a small increase in grafting content can be measured after  
 254 24 hours of reaction, however the average molecular weight of the produced homopolymer started  
 255 decreasing, showing potential signs of depolymerization or transcarbonation reactions. Therefore 5 hours  
 256 was the favoured reaction time for most reaction, as it allowed for a good control over grafting while having  
 257 good conversion, and a very good reproducibility (repeated reactions available in SI).

258 At the typical ratio of TMC/Cat/OH of 500/1/50, variation in temperature was tested to determine its  
259 influence on the grafting reaction. At first glance, the temperature did not appear to change the amount of  
260 grafting by a significant amount, as increasing the temperature to 40°C (entry 14) or 60°C (entry 15) yielded  
261 CNCs with 51% and 52% grafts respectively (compared to entry 2). However, at temperatures as low as  
262 40°C, browning of the CNCs was observed and became more pronounced at higher temperature, indicating  
263 a potential degradation of the material. A shortening of the homopolymer chains is further observed as the  
264 reaction temperature increases, indicating of possible depolymerization / chain scission reactions in the  
265 presence of TBD, which has been reported for both polycarbonates (Li, Sablong, van Benthem, & Koning,  
266 2017) and polylactides (Meimoun et al., 2020). A reaction at 0°C was also performed using an ice bath to  
267 determine if a lower temperature could favour grafting over homopolymerization (entry 13), however the  
268 results obtained for the grafting of CNC were in the same range (>50%) as the reaction performed at room  
269 temperature (RT). The temperature used for the rest of the reaction was therefore set to RT (controlled by  
270 an oil bath) to avoid any degradation of the material and to keep the reaction more energy efficient.

271 A reaction was then performed under inert atmosphere, but not under glovebox conditions, to evaluate how  
272 sensitive the efficiency of the grafting was regarding the presence of water and other impurities (entry 16).  
273 Prior to the reaction, CNCs and TMC were dried using a vacuum and an argon line rather than ultra-high  
274 vacuum. THF was used after purification over alumina, similarly to experiments performed inside the  
275 glovebox. Multiple argon/vacuum cycles were used to ensure inert atmosphere was achieved. Under these  
276 conditions, a low amount of grafting (7 vs. 51% in entry 2) as well as the short chain length of the  
277 homopolymer (impossible to precipitate in cold methanol) showed the prevalence of initiation by traces of  
278 water and ethanol. Due to CNCs being hydrophilic, it is hard to remove significant traces of water from  
279 them without extreme conditions ( $10^{-6}$  bar of vacuum), as well as ethanol from the purification steps of  
280 preparing CNCs. This reaction shows that in order to maximize grafting efficiency purification of the  
281 different chemicals a thorough drying of the cellulose is required, and working in a glovebox is useful.

282 In an attempt to increase grafting on cellulose, reactions were then performed with an increased ratio of  
283 TMC/CNC by decreasing the quantity of cellulose used. Surprisingly, increasing the quantity of monomer  
284 did not lead to a significant improvement in the grafting amount on cellulose (entries 17-18), which seems  
285 to reach a maximum at around 50%, a result similar to other reactions (entry 2). This shows that simply  
286 increasing the quantity of monomer used in the reaction is an ineffective way to increase the maximum  
287 amount of grafting on the surface of CNC.

288 To determine if the availability of the hydroxyl groups on the surface of cellulose is an important factor, a  
289 reaction was performed on a batch of CNC in THF with increased effort at individualization of CNCs. The  
290 mixture of cellulose and solvent was prepared in the glovebox, then closed tightly and stirred over 24 hours

291 vs. 30 min previously used. A sonication bath was also used in burst of 5 minutes over the 24 hours. The  
292 results obtained (entry 19) when compared to a “typical” reaction showed that increased effort for maximum  
293 individualization of CNCs did not have a significant impact as the grafting obtained was also around the  
294 50% mark.

295 The influence of catalyst loading was further assessed. Using a typical ratio TMC/TBD/OH of 500/1/50  
296 showed good results and a grafting of around 50%. Increasing the catalyst ratio to 2 equivalents vs. OH  
297 (entry 20) however lowered the grafting % on CNCs by a significant amount, whereas the length of the  
298 homopolymer increased, indicating that increasing the TBD amount favours homopolymerization.  
299 Increasing the amount of catalyst further to 5 equivalents (entry 21) yielded a similar amount of grafting  
300 onto the CNCs than entry 20 (9%), but the average molecular weight of the isolated polymer was  
301 significantly smaller ( $< 3000 \text{ g.mol}^{-1}$ ). As mentioned previously, TBD is not only capable of polymerization,  
302 but also depolymerization under the right circumstances *via* a nucleophilic attack on the carbonyl moieties  
303 (Meimoun *et al.* 2020). In the case of polylactide, the use of 5 equivalents of TBD decreased the average  
304 molecular of the resulting polymer more than tenfold, a result very similar to what is observed in this work  
305 for the polycarbonate.

306 As opposed to increasing the catalyst quantity, lowering the amount of TBD used for the reaction to 0.5  
307 equivalents showed an improvement in the grafting on CNCs with a material composed of up to 74%  
308 polycarbonate grafts by weight and a grafting yield of 46% (entry 22).  $M_n$  of the homopolymer obtained  
309 was lower, which can simply be explained by the increased quantity of monomer turned into grafts rather  
310 than homopolymer.

311 Decreasing the quantity of catalyst further resulted in a decrease in the amount of grafting to 64% (entry  
312 23), which is an improvement over the result obtained with 1 equivalent (entry 2) but a setback compared  
313 to reactions performed with 0.5 equivalent (entry 22). Moreover, the low concentration of TBD led to a  
314 slower reaction, and obtaining full conversion became more difficult.

315 To improve the grafting efficiency with respect to the total amount of monomer used, reactions with 0.5  
316 equivalent of TBD (shown to have the best results) and successively lower amounts of monomer were  
317 carried out.

318 The grafting % decreased from 74% to 57% (entry 22 vs. 24) when the monomer concentration was halved,  
319 but the grafting yield stayed within the same range at 42%. While this is not an improvement, it however,  
320 allows one to obtain CNCs with around 50% grafts with significantly less monomer loss than some previous  
321 experiments (*e.g* entry 2). Lowering the amount of monomer further continued to reduce the % grafting

322 (47%) but led to an increased yield of 56% which is a good value for grafting of a polymer on cellulose, as  
323 this parameter is usually overlooked in favour of trying to reach a maximum amount of grafting.

324 A similar reaction was also performed with a typical 1 equivalent TBD to compare to the grafting yield  
325 obtained with 0.5 equivalents. As previously shown, the grafting % obtained is superior using a lower  
326 quantity of catalyst, leading to a higher grafting yield.

327 Overall, this shows that a wide range of grafting % is possible, and specific values can be targeted using the  
328 right amount of catalyst (typically 0.5 eq) without having to use a large excess of monomer, while keeping  
329 the grafting yield as high as possible.

### 330 3.3. Characterization of the poly(trimethylene carbonate)-grafted CNC as a function of 331 the grafting ratio

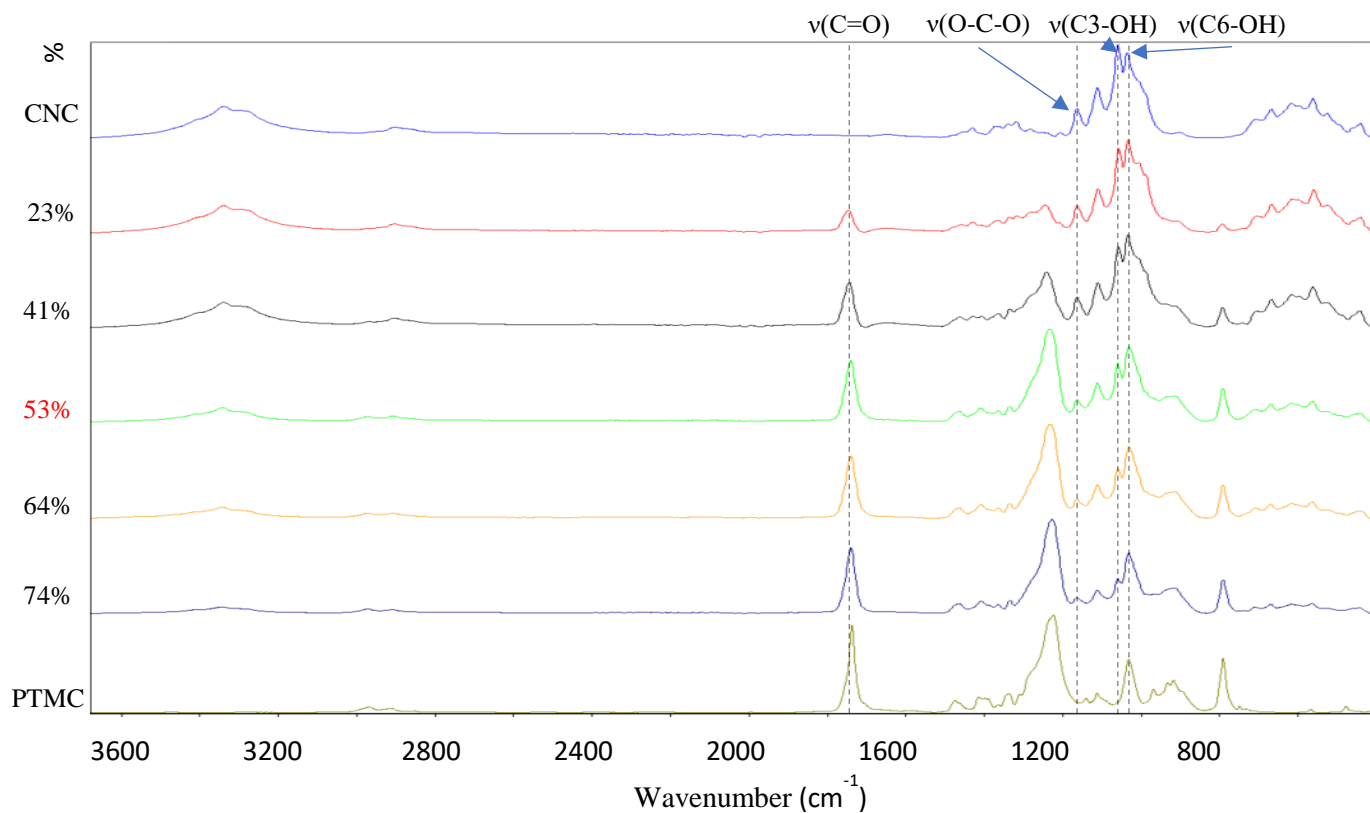


Figure 3: FT-IR spectra of unmodified cellulose nanocrystals (CNC) and grafted one with different graft content after purification by Soxhlet extraction. PTMC of 154000 g/mol extracted from soxhlet and purified by precipitation. Grafted CNCs corresponding to refer

332  
333 In addition to elemental analysis, FT-IR was used to determine the success of the grafting reaction (Figure  
334 3). As expected, both modified and unmodified cellulose spectra resemble each other. However, 2 bands  
335 characteristic to our grafts are visible for modified cellulose. First, the band at 1754 cm<sup>-1</sup> can be identified

336 as a carbonyl stretch  $\nu(\text{C}=\text{O})$ , thus confirming the successful incorporation of the carbonate moieties onto  
337 CNCs. A second characteristic band is observed at  $1229\text{ cm}^{-1}$  corresponding to  $\nu(\text{C}-\text{O})$  stretching (Nyquist  
338 & Potts, 1961). As shown in Figure 3, the relative intensity of both bands increased with the grafting content,  
339 thus confirming the results determined by elemental analysis and TGA. Lastly, the ratio of absorption band  
340 at  $1059\text{ cm}^{-1}$  corresponding to  $\nu(\text{C}3-\text{OH})$  to C-O-C stretching at  $1160\text{ cm}^{-1}$  (Marechal & Chanzy, 2000),  
341 decreases with increasing grafting ratio which shows the successful esterification of the secondary alcohol  
342 in the C3 position. The band at  $1032\text{ cm}^{-1}$  corresponding to  $\nu(\text{C}6-\text{OH})$  increases with increasing grafting  
343 ratio, as terminal OH of the polycarbonate chains appear in this region as well. As a consequence, grafting  
344 on the C6 position is not “visible” by FTIR, as both primary and secondary C-OH of cellulose are replaced  
345 by the primary terminal C-OH of the polymer at  $1032\text{ cm}^{-1}$ . Note that  $\nu(\text{C}2-\text{OH})$  cannot be discussed here  
346 as the polymer has a band in the area.

347 X-ray photoelectron spectroscopy can give additional insight into the composition of the modified CNCs at

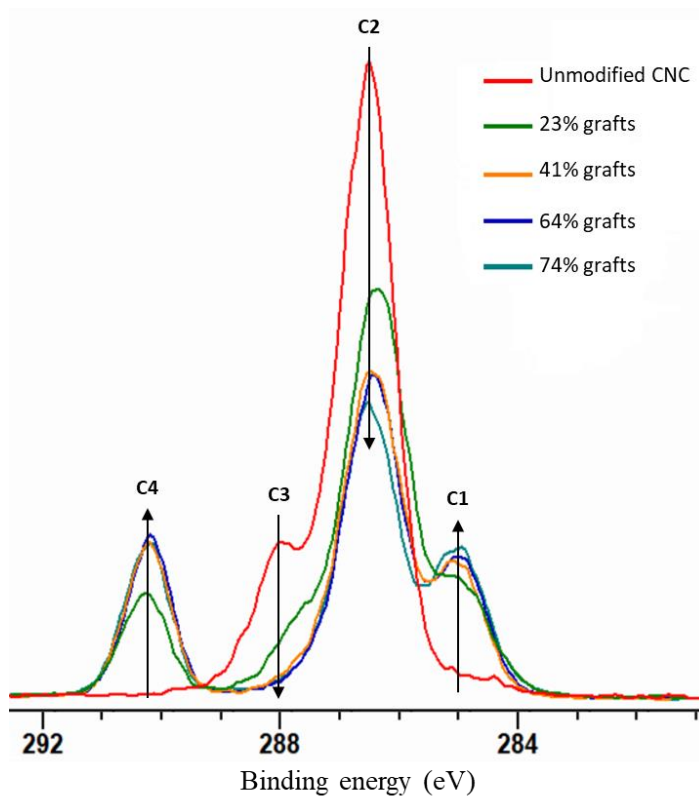
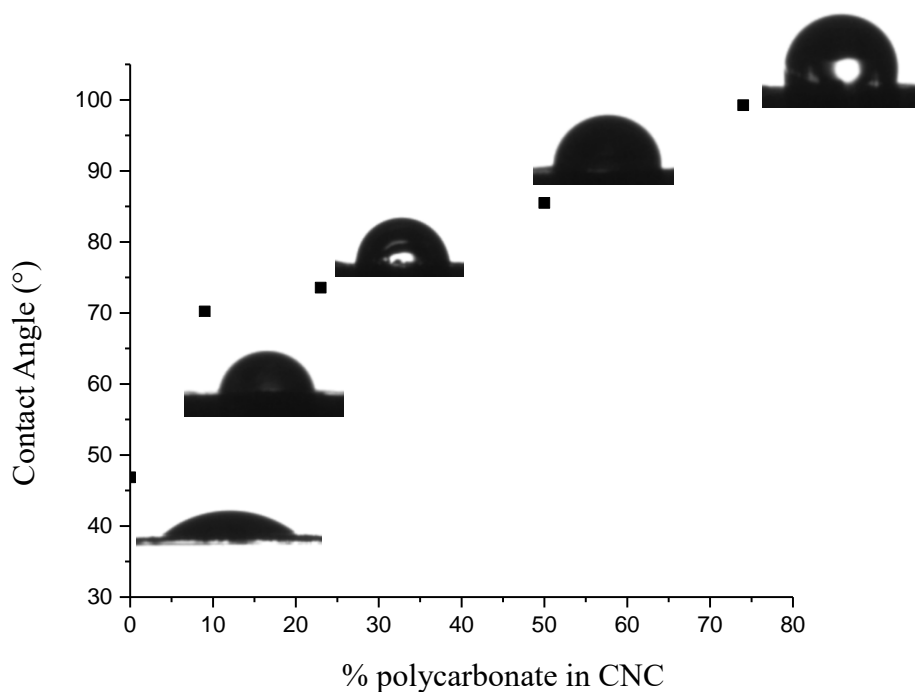


Figure 4: Carbon 1s X-ray photoelectron spectroscopy (XPS) scan of cellulose nanocrystals grafted with different poly(trimethylene carbonate content). Grafted CNCs corresponding to reference in Table 2: entry 26 (23%) entry 28 (41%), entry 23 (64%), entry 22 (74%)

348 a surface level. In the C1s high resolution scan (Figure 4), the aliphatic C-C carbon contribution (C1) at 285  
349 eV is shown to increase rapidly with grafting, as cellulose units do not contain aliphatic carbons, unlike  
350 trimethylene carbonate. With an increasing amount of graft content, the relative intensity of the C1

351 contribution increases and then appears to reach a maximum, at the contribution amount expected for pure  
352 poly(trimethylene carbonate) chains indicating that no cellulose contribution is visible anymore. As opposed  
353 to C1, the C2 and C3 contributions to the C1s signal, corresponding to C-O and O-C-O environments  
354 respectively, both decreased with an increasing amount of grafts, as poly(trimethylene carbonate)  
355 contributes less to the C-O signal than cellulose, and does not contribute to the O-C-O signal. Finally, the  
356 O-C=O contribution (C4) increased with grafting content, similarly to C1 as the carbonate function is the  
357 only contribution to this peak. The results obtained from elemental analysis, along with form of  
358 characterization are therefore confirmed with the XPS data.

359 With poly(trimethylene carbonate) being a highly hydrophobic material, grafting CNCs with it will change  
360 its interaction with water significantly. To quantify this, grafted CNCs were used in contact angle



*Figure 5: Contact angle of a water droplet on the surface of CNC modified with different polycarbonate content. Grafted CNCs corresponding to reference in Table 2: entry 9 (9%) entry 26 (23%), entry 2 (51%), and entry 22 (74%)*

361 measurements with water. The water contact angle increased rapidly with the poly(trimethylene carbonate)  
362 content of the cellulose sample (Figure 5), in line with the length of the graft in the brush copolymer  
363 structure. For a poly(trimethylene carbonate) content as low as 9%, the increase in hydrophobicity is  
364 significant, which then increases more slowly as the carbonate content increased, up to a value close to that  
365 of pure PTMC reported in the range 90-110°C (Brossier et al., 2021; Yao et al., 2017). This might be related  
366 to an increasing coverage of the CNC by PTMC, ranging from partial to almost full. It is noteworthy that  
367 the contact angle and thus the wettability can be controlled by targeting the proper polycarbonate grafting

368 ratio. As a result, we believe that this increase in hydrophobicity shows good signs for the potential  
369 incorporation of these nanoparticles in a polymer matrix for composite applications.

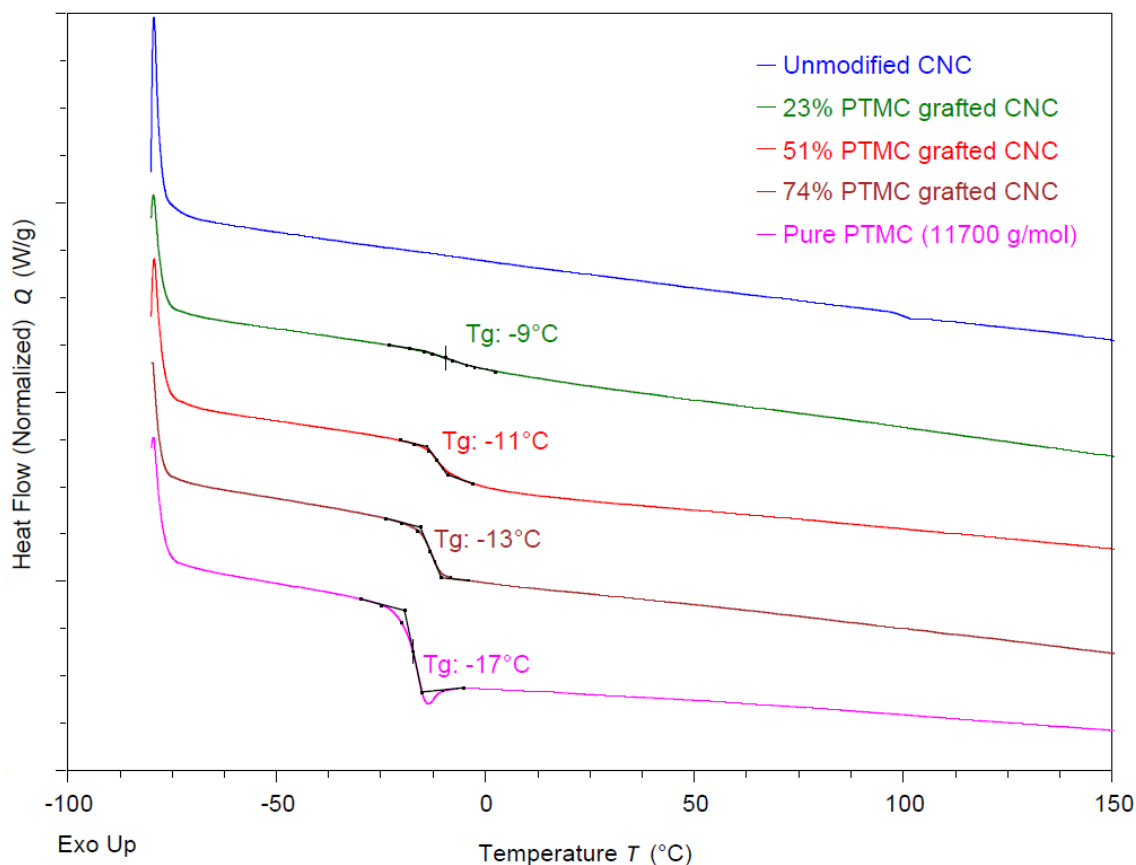


Figure 6: Differential Scanning Calorimetry graphs of CNC, poly(trimethylene carbonate) (PTMC) and modified CNC during the second heating at 10°C/min. . Grafted CNCs corresponding to reference in Table 2: entry 26 (23%), entry 2 (51%), and entry 22 (74%)

370 DSC analyses were conducted to obtain more information on the thermal behaviour of the grafts. The  
371 samples were heated from -80 to 190°C, as the glass transition temperature ( $T_g$ ) of poly(trimethylene  
372 carbonate) is below 0 °C. For unmodified CNCs, no  $T_g$  or melting point were observed, as expected (Figure  
373 6Figure 6). For grafted CNCs, a glass transition was observed for all samples in the same range as the  $T_g$  of  
374 pure poly(trimethylene carbonate), but with slightly higher values. With a graft content as low as 23%, a  $T_g$   
375 at -9°C can be recorded, indicative of the presence of poly(trimethylene carbonate) grafts. As the carbonate  
376 content increased, the  $T_g$  decreased and progressively moved towards the value for poly(trimethylene  
377 carbonate) homopolymer (11700 g.mol<sup>-1</sup>) at -17°C, without ever reaching it. This phenomenon could be  
378 attributed to a lower mobility of the chain closer to the CNC backbone, their relative amount decreasing  
379 with higher grafting values. Overall, this shows that polymer grafts on cellulose nanocrystals are of  
380 sufficient length to showcase polymeric behaviour. In addition, we also measured the  $T_g$  of non-grafted  
381 homopolymers of similar molecular weight and compared it with that of the grafted polymer (see SI section



382 S12). The 3 homopolymers of *ca.* 20 000 g/mol show a  $T_g$  of *ca.* -16/-17 °C, whereas the  $T_g$  of the grafted  
383 CNC are in the range -10 to -13°C, which tend to confirm the occurrence of a true grafting.

384 In order to know whether the cellulose nanocrystals retain their structure following grafting, wide-angle X-  
385 ray scattering was used to determine the crystallinity of the pristine and PTMC grafted CNC samples. The  
386 X-ray scattering data was fitted with the crystal structure of cellulose I $\beta$ , and the amorphous contribution to  
387 the scattering determined. As no melting peak was seen in the DSC data, we know that the PTMC will be  
388 included in the amorphous contribution to the scattering data. Therefore, considering the amount of PTMC  
389 in the sample, changes in crystallinity of the cellulose ( $\Delta\chi_{c, \text{cellulose}}$ ) can be determined as the difference in  
390 crystallinity between the starting material and the product ( $\Delta\chi_{c, \text{sample}}$ ), minus the expected contribution from  
391 PTMC ( $\phi_{\text{PTMC}}$  – the volume fraction of PTMC) as shown in Table 3.

392 *Table 3: The calculated sample crystallinity based on WAXS measurements for all samples*

Sample	$\chi_{c, \text{sample}}$	$\Delta\chi_{c, \text{sample}}$	$\phi_{\text{PTMC}}$	$\Delta\chi_{c, \text{cellulose}}$
Unmodified CNC	0.99	-	0	0
23% PTMC-g-CNC	0.68	-0.31	0.27	-0.04
41% PTMC-g-CNC	0.56	-0.43	0.46	0.03
51% PTMC-g-CNC	0.37	-0.62	0.56	-0.06
64% PTMC-g-CNC	0.26	-0.73	0.69	-0.04
74% PTMC-g-CNC	0.14	-0.85	0.78	-0.07

393 The data on the grafted samples shows only around 5% change in cellulose crystallinity when the  
394 contribution from amorphous PTMC is removed. This change could be due to peeling of the surface chains  
395 of the CNC during grafting, however, given the lack of trend in  $\Delta\chi_{c, \text{cellulose}}$ , and the wide standard deviation  
396 in the values, it is possible that this reflects the error in the calculation of the sample crystallinity by this  
397 methodology.

398

## 399 Conclusion

400 Ring-opening polymerization (ROP) of trimethylene carbonate was performed using cellulose nanocrystals  
401 as a co-initiator in the presence of 4 organocatalysts, *i.e.* DMAP, DBU, TBD and BEMP). The overall  
402 performances considering conversion, grafting ratio and yield are TBD > BEMP > DBU, DMAP. After  
403 optimization, a grafting ratio as high as 74% could be reached using TBD, corresponding to a material  
404 composed by weight of almost  $\frac{3}{4}$  polycarbonate grafts. The reaction was performed at room temperature  
405 with a low concentration of the catalyst, 0.5% vs. TMC and 500 equiv. TMC per glucose unit. This led to a

406 material with  $T_g$  and contact angle close to that of poly(trimethylene carbonate). The use of a single step  
407 reaction, under mild conditions while keeping grafting yield high is of great interest to produce CNC with  
408 a controlled amount of grafts. Furthermore, we were able to show some of the most influential parameters  
409 with respect to grafting content, providing some insight on the chemistry behind cellulose modification. The  
410 contact angle can be tuned from *ca.* 50 to 100° by adjusting the grafting ratio. Lastly, DSC results revealed  
411 the polymeric behaviour of the grafts, confirming the successful grafting of polycarbonate chains of  
412 sufficient length to have high potential as reinforcement fillers in composite materials. To our knowledge,  
413 this is the first reported chemical modification of cellulose nanocrystals with trimethylene carbonate, and  
414 the first example of a ROP-based grafting from process attaching polycarbonate chains onto CNCs.

415

#### 416 **4. Acknowledgement**

417 The authors are grateful to Aurélie Malfait for SEC measurements, and Gertrude Kignelman for the help  
418 with contact angle analysis. The authors also acknowledge financial support from the Initiatives for  
419 Science, Innovation, Territories and Economy (I-SITE) Lille Nord – Europe (MLT PhD fellowship), from  
420 Research Foundation Flanders (grant G0C6013N), KU Leuven (grant C14/18/061) and from the European  
421 Union’s European Fund for Regional Development, Flanders Innovation & Entrepreneurship, and the  
422 Province of West-Flanders for financial support in the Accelerate<sup>3</sup> project (Interreg Vlaanderen-Nederland  
423 program). Université de Lille, Chevreul Institute (FR 2638), Ministère de l’Enseignement Supérieur de la  
424 Recherche et de l’Innovation, Région Hauts de France are also acknowledged for supporting and funding  
425 partially this work.

426

427 **5. References:**

- 428  
429  
430 Albertsson, A.-C., & Varma, I. K. (2003). Recent Developments in Ring Opening Polymerization of  
431 Lactones for Biomedical Applications. *Biomacromolecules*, 4(6), 1466–1486.
- 432 Anžlovar, A., Krajnc, A., & Žagar, E. (2020). Silane modified cellulose nanocrystals and nanocomposites  
433 with LLDPE prepared by melt processing. *Cellulose*, 27(10), 5785–5800.
- 434 Artham, T., & Doble, M. (2008). Biodegradation of Aliphatic and Aromatic Polycarbonates:  
435 Biodegradation of Aliphatic and Aromatic Polycarbonates. *Macromolecular Bioscience*, 8(1), 14–24.
- 436 Azzam, F., Heux, L., & Jean, B. (2016). Adjustment of the Chiral Nematic Phase Properties of Cellulose  
437 Nanocrystals by Polymer Grafting. *Langmuir*, 32(17), 4305–4312.
- 438 Brossier, T., Volpi, G., Vasquez-Villegas, J., Petitjean, N., Guillaume, O., Lapinte, V., & Blanquer, S.  
439 (2021). Photoprintable Gelatin- *graft* -Poly(trimethylene carbonate) by Stereolithography for Tissue  
440 Engineering Applications. *Biomacromolecules*, 22(9), 3873–3883.
- 441 Dufresne, A. (2013). Nanocellulose: a new ageless bionanomaterial. *Materials Today*, 16(6), 220–227.
- 442 Engler, A. C., Chan, J. M. W., Fukushima, K., Coady, D. J., Yang, Y. Y., & Hedrick, J. L. (2013).  
443 Polycarbonate-Based Brush Polymers with Detachable Disulfide-Linked Side Chains. *ACS Macro Letters*,  
444 2(4), 332–336.
- 445 Eyley, S., & Thielemans, W. (2014). Surface modification of cellulose nanocrystals. *Nanoscale*, 6(14),  
446 7764–7779.
- 447 Favier, V., Chanzy, H., & Cavaille, J. Y. (1995). Polymer Nanocomposites Reinforced by Cellulose  
448 Whiskers. *Macromolecules*, 28(18), 6365–6367.
- 449 Girouard, N. M., Xu, S., Schueneman, G. T., Shofner, M. L., & Meredith, J. C. (2016). Site-Selective  
450 Modification of Cellulose Nanocrystals with Isophorone Diisocyanate and Formation of Polyurethane-CNC  
451 Composites. *ACS Applied Materials & Interfaces*, 8(2), 1458–1467.
- 452 Habibi, Y. (2014). Key advances in the chemical modification of nanocelluloses. *Chem. Soc. Rev.*, 43(5),  
453 1519–1542.

454 Habibi, Y., Goffin, A.-L., Schiltz, N., Duquesne, E., Dubois, P., & Dufresne, A. (2008). Bionanocomposites  
455 based on poly( $\epsilon$ -caprolactone)-grafted cellulose nanocrystals by ring-opening polymerization. *Journal of*  
456 *Materials Chemistry*, 18(41), 5002.

457 Habibi, Y., Lucia, L. A., & Rojas, O. J. (2010). Cellulose Nanocrystals: Chemistry, Self-Assembly, and  
458 Applications. *Chemical Reviews*, 110(6), 3479–3500.

459 Hafrén, J., & Córdova, A. (2005). Direct Organocatalytic Polymerization from Cellulose Fibers: Direct  
460 Organocatalytic Polymerization from Cellulose Fibers. *Macromolecular Rapid Communications*, 26(2), 82–  
461 86.

462 Helou, M., Miserque, O., Brusson, J.-M., Carpentier, J.-F., & Guillaume, S. M. (2010). Organocatalysts for  
463 the Controlled “Immortal” Ring-Opening Polymerization of Six-Membered-Ring Cyclic Carbonates: A  
464 Metal-Free, Green Process. *Chemistry - A European Journal*, 16(46), 13805–13813.

465 Helou, M., Miserque, O., Brusson, J.-M., Carpentier, J.-F., & Guillaume, S. M. (2008). Ultraproductive,  
466 Zinc-Mediated, Immortal Ring-Opening Polymerization of Trimethylene Carbonate. *Chemistry - A*  
467 *European Journal*, 14(29), 8772–8775.

468 Ishikawa T, editor. Superbases for organic synthesis: guanidines, amidines and phosphazenes and related  
469 organocatalysts. Chichester: John Wiley & Sons, Ltd; 2009; 336 pp

470 Jerome, C., & Lecomte, P. (2008). Recent advances in the synthesis of aliphatic polyesters by ring-opening  
471 polymerization. *Advanced Drug Delivery Reviews*, 60(9), 1056–1076.

472 Kaljurand, I., Kütt, A., Sooväli, L., Rodima, T., Mäemets, V., Leito, I., & Koppel, I. A. (2005). Extension  
473 of the Self-Consistent Spectrophotometric Basicity Scale in Acetonitrile to a Full Span of 28 p K a Units:  
474 Unification of Different Basicity Scales. *The Journal of Organic Chemistry*, 70(3), 1019–1028.

475 Kamber, N. E., Jeong, W., Waymouth, R. M., Pratt, R. C., Lohmeijer, B. G. G., & Hedrick, J. L. (2007).  
476 Organocatalytic Ring-Opening Polymerization. *Chemical Reviews*, 107(12), 5813–5840.

477 Kluin, O. S., van der Mei, H. C., Busscher, H. J., & Neut, D. (2009). A surface-eroding antibiotic delivery  
478 system based on poly-(trimethylene carbonate). *Biomaterials*, 30(27), 4738–4742.

479 Labet, M., & Thielemans, W. (2011). Improving the reproducibility of chemical reactions on the surface  
480 of cellulose nanocrystals: ROP of  $\epsilon$ -caprolactone as a case study. *Cellulose*, 18(3), 607–617.

481 Labet, M., & Thielemans, W. (2012). Citric acid as a benign alternative to metal catalysts for the production  
482 of cellulose-grafted-polycaprolactone copolymers. *Polymer Chemistry*, 3(3), 679

483 Lalanne-Tisné, M., Mees, M. A., Eyley, S., Zinck, P., & Thielemans, W. (2020). Organocatalyzed ring  
484 opening polymerization of lactide from the surface of cellulose nanofibrils. *Carbohydrate Polymers*, 250,  
485 116974.

486 Lasseguette, E. (2008). Grafting onto microfibrils of native cellulose. *Cellulose*, 15(4), 571–580.

487 Lendlein, A., Langer R. (2002). Biodegradable, Elastic Shape-Memory Polymers for Potential Biomedical  
488 Applications. *Science*, 296(5573), 1673–1676.

489 Li, C., Sablong, R. J., van Benthem, R. A. T. M., & Koning, C. E. (2017). Unique Base-Initiated  
490 Depolymerization of Limonene-Derived Polycarbonates. *ACS Macro Letters*, 6(7), 684–688.

491 Lohmeijer, B. G. G., Pratt, R. C., Leibfarth, F., Logan, J. W., Long, D. A., Dove, A. P., Nederberg, F., Choi,  
492 J., Wade, C., Waymouth, R. M., & Hedrick, J. L. (2006). Guanidine and Amidine Organocatalysts for Ring-  
493 Opening Polymerization of Cyclic Esters. *Macromolecules*, 39(25), 8574–8583.

494 Marechal, Y., & Chanzy, H. (2000). The hydrogen bond network in Ib cellulose as observed by infrared  
495 spectrometry. *Journal of Molecular Structure*, 14.

496 Meimoun, J., Favrelle-Huret, A., Bria, M., Merle, N., Stoclet, G., De Winter, J., Mincheva, R., Raquez, J.-  
497 M., & Zinck, P. (2020). Epimerization and chain scission of polylactides in the presence of an organic base,  
498 TBD. *Polymer Degradation and Stability*, 181, 109188.

499 Miao, C., & Hamad, W. Y. (2016). In-situ polymerized cellulose nanocrystals (CNC)—poly( l -lactide)  
500 (PLLA) nanomaterials and applications in nanocomposite processing. *Carbohydrate Polymers*, 153, 549–  
501 558.

502 Nederberg, F., Lohmeijer, B. G. G., Leibfarth, F., Pratt, R. C., Choi, J., Dove, A. P., Waymouth, R. M., &  
503 Hedrick, J. L. (2007). Organocatalytic Ring Opening Polymerization of Trimethylene Carbonate.  
504 *Biomacromolecules*, 8(1), 153–160.

505 Nyquist, R. A., & Potts, W. J. (1961). Infrared absorptions of organic carbonate derivatives and related  
506 compounds. *Spectrochimie Acts*, 17, 679-697.

507 Ottou, W. N., Sardon, H., Mecerreyes, D., Vignolle, J., & Taton, D. (2016). Update and challenges in  
508 organo-mediated polymerization reactions. *Progress in Polymer Science*, 56, 64–115.

509 Ottou, W. N., Sardon, H., Mecerreyes, D., Vignolle, J., & Taton, D. (2016). Update and challenges in  
510 organo-mediated polymerization reactions. *Progress in Polymer Science*, 56, 64–115.

511 Palard, I., Schappacher, M., Belloncle, B., Soum, A., & Guillaume, S. M. (2007). Unprecedented  
512 Polymerization of Trimethylene Carbonate Initiated by a Samarium Borohydride Complex: Mechanistic  
513 Insights and Copolymerization with  $\epsilon$ -Caprolactone. *Chemistry - A European Journal*, 13(5), 1511–1521.

514 Park, S.-A., Eom, Y., Jeon, H., Koo, J. M., Lee, E. S., Jegal, J., Hwang, S. Y., Oh, D. X., & Park, J. (2019).  
515 Preparation of synergistically reinforced transparent bio-polycarbonate nanocomposites with highly  
516 dispersed cellulose nanocrystals. *Green Chemistry*, 21(19), 5212–5221.

517 Penczek, S., Cypryk, M., Duda, A., Kubisa, P., & Slomkowski, S. (2007). Living ring-opening  
518 polymerizations of heterocyclic monomers. *Progress in Polymer Science*, 32(2), 247–28

519 Pendergraph, S. A., Klein, G., Johansson, M. K. G., & Carlmark, A. (2014). Mild and rapid surface initiated  
520 ring-opening polymerisation of trimethylene carbonate from cellulose. *RSC Advances*, 4(40), 20737.

521 Revol, J.-F., Bradford, H., Giasson, J., Marchessault, R. H., & Gray, D. G. (1992). Helicoidal self-ordering  
522 of cellulose microfibrils in aqueous suspension. *International Journal of Biological Macromolecules*, 14(3),  
523 170–172.

524 Sahlin, K., Forsgren, L., Moberg, T., Bernin, D., Rigdahl, M., & Westman, G. (2018). Surface treatment of  
525 cellulose nanocrystals (CNC): effects on dispersion rheology. *Cellulose*, 25(1), 331–345.

526 Samuel, C., Chalamet, Y., Boisson, F., Majesté, J.-C., Becquart, F., & Fleury, E. (2014). Highly efficient  
527 metal-free organic catalysts to design new Environmentally-friendly starch-based blends. *Journal of*  
528 *Polymer Science Part A: Polymer Chemistry*, 52(4), 493–503.

529 Simón, L., & Goodman, J. M. (2007). The Mechanism of TBD-Catalyzed Ring-Opening Polymerization of  
530 Cyclic Esters. *The Journal of Organic Chemistry*, 72(25), 9656–9662.

531 Stanley, N., Chenal, T., Jacquel, N., Saint-Loup, R., Prates Ramalho, J. P., & Zinck, P. (2019).  
532 Organocatalysts for the Synthesis of Poly(ethylene terephthalate-*co*-isosorbide terephthalate): A Combined  
533 Experimental and DFT Study. *Macromolecular Materials and Engineering*, 304(9), 1900298.

534 Thielemans, W., Belgacem, M. N., & Dufresne, A. (2006). Starch Nanocrystals with Large Chain Surface  
535 Modifications. *Langmuir*, 22(10), 4804–4810.

536 Trinh, B. M., & Mekonnen, T. (2018). Hydrophobic esterification of cellulose nanocrystals for epoxy  
537 reinforcement. *Polymer*, 155, 64–74.

538 Wohlhauser, S., Delepierre, G., Labet, M., Morandi, G., Thielemans, W., Weder, C., & Zoppe, J. O. (2018).  
539 Grafting Polymers *from* Cellulose Nanocrystals: Synthesis, Properties, and Applications. *Macromolecules*,  
540 *51*(16), 6157–6189.

541 Xu, J., Wu, Z., Wu, Q., & Kuang, Y. (2020). Acetylated cellulose nanocrystals with high-crystallinity  
542 obtained by one-step reaction from the traditional acetylation of cellulose. *Carbohydrate Polymers*, *229*,  
543 115553.

544 Yao, H., Li, J., Li, N., Wang, K., Li, X., & Wang, J. (2017). Surface Modification of Cardiovascular Stent  
545 Material 316L SS with Estradiol-Loaded Poly (trimethylene carbonate) Film for Better Biocompatibility.  
546 *Polymers*, *9*(11), 598.

547 Yu, W., E. Maynard, Chiaradia, V., Arno, M.C., Dove, A.P. (2021) Aliphatic Polycarbonates from Cyclic  
548 Carbonate Monomers and Their Application as Biomaterials, *Chemical Reviews*, *121*, 10865–10907.

549

550

551